

# Nonlinear current response of micro electroporation and resealing dynamics for human cancer cells

Huiqi He<sup>a</sup>, Donald C. Chang<sup>c</sup>, Yi-Kuen Lee<sup>a,b,\*</sup>

<sup>a</sup> Bioengineering Graduate Program, The Hong Kong University of Science and Technology, Clear Water Bay, Kowloon, Hong Kong

<sup>b</sup> Department of Mechanical Engineering, The Hong Kong University of Science and Technology, Clear Water Bay, Kowloon, Hong Kong

<sup>c</sup> Department of Biology, The Hong Kong University of Science and Technology, Clear Water Bay, Kowloon, Hong Kong

Received 24 October 2007; accepted 11 January 2008

Available online 29 January 2008

## Abstract

This paper presents a novel method to measure the dynamic process of membrane permeability during electroporation (EP) on microchips for human cancer cells. Micro EP chips with three-dimensional gold electrodes accommodating a single cell in between were fabricated with a modified electroplating process. Electrochemical impedance spectroscopy (EIS) was carried out with an electrochemistry analyzer on micro EP chips and a nonlinear equivalent circuit model was proposed to describe the dynamic response of the whole system. Using such a method, micro EP current was isolated from undesired leakage current to study the corresponding electroporation dynamics under different input voltages. In addition, cell membrane recovery dynamics after electroporation was also studied and the resealing time constants were determined for different pulse treatments. © 2008 Elsevier B.V. All rights reserved.

**Keywords:** Electroporation; Electric current response; MEMS; HeLa cell; Equivalent circuit

## 1. Introduction

Membrane electroporation (EP) is the use of an intense electric pulse to make the cell membrane transiently porous and then permeable to exogenous molecules present in the surrounding media [1,2]. It has been shown that electric field controls the permeabilization of cell membrane in two ways [3]. The pulse amplitude determines the electric field intensity which initiates the short-lived structural changes in the cell membrane, while the pulse duration provides time to allow the initiated pore size to expand. The permeability of the cell membrane and the resealing dynamics can be quantified by fluorescence microscopy [4]. The electroporation efficiency, i.e., the uptake of different size molecules by cells, has been studied under various electric pulse amplitudes and durations [5,6]. In addition, the

measurements of the electrical properties change of the cells during and after electroporation, such as transmembrane voltage  $U_m(t)$ , transmembrane current  $I_m(t)$  [7] or conductometric and electrooptic relaxation spectrometry [8,9], provided another way to characterize the dynamics of cell membrane permeability.

The electric current in response to electroporation on micro EP chips  $I_{tot}$  mainly consists of the electroporation currents (transmembrane currents)  $I_{EP}$ , the leakage currents  $I_{Leak}$  (including the membrane capacitance currents  $I_{cap}$  and the currents bypassing cells  $I_{bypass}$ ) and the ion-channel currents  $I_{ion}$ , as illustrated in Fig. 1. The application of an external electric field to the cell results in a considerable increase in the membrane conductance. The EP current is directly related to membrane conductivity change which is induced by the initiation of nanometer-scaled pore. However, it is very difficult to observe the dynamics of these pores using a regular fluorescence microscope.

Kinosita and Tsong have shown that electric field pulses ( $1.5 \text{ kV/cm} \leq E \leq 6 \text{ kV/cm}$  and  $80 \mu\text{s}$  pulse duration) significantly increase the conductivity of erythrocyte suspension in 1979 [10]. However, this kind of conductivity change can only be measured in a low conductivity solution (use sucrose as the one of the main

\* Corresponding author. Department of Mechanical Engineering, HKUST, Clear Water Bay, Kowloon, Hong Kong. Tel.: +852 2358 8663; fax: +852 2358 1543.

E-mail address: [meyklee@ust.hk](mailto:meyklee@ust.hk) (Y.-K. Lee).

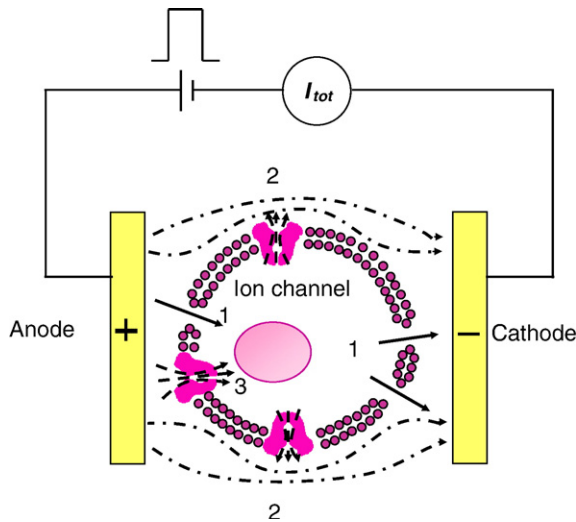


Fig. 1. Schematic diagram of three electric current components on micro electroporation chip. 1. EP current  $I_{EP}$  (solid line), 2. Leakage current  $I_{Leak}$  (dash dot) (include bypassing current and capacitor current), 3. Ion-channel current  $I_{ion}$  (dash line).  $I_{tot} = I_{Leak} + I_{ion} + I_{EP}$

solvents), which is different from a commonly used electroporation buffer.

Recently, Ryttsen et al. [11] and Krassen et al. [12] used the patch-clamp technique to measure the nonlinear current–voltage relationship of a single cell. Gowrishankar et al. immobilized a single muscle fiber between a double vaseline gap voltage-clamp for studying the dynamics of electroporation and resealing [13]. These types of experiments connected the cell membrane with a pipette or patch-clamp to ensure a tight seal. In this case, the leakage current could be neglected. However, the manipulation of the cells using a pipette causes difficulties in operation and usually requires complicated instrumentation.

In order to have a deeper understanding about EP, the electric current monitoring during electric field can be used to study membrane electroporation, circumventing the limitation of optical method. Since the total current response recorded from micro EP chip consists of three components:

$$I_{tot} = I_{Leak} + I_{ion} + I_{EP}, \quad (1)$$

the EP current  $I_{EP}$  needs to be isolated from the other currents (i.e.  $I_{Leak}$  and  $I_{ion}$ ). Usually, the ion-channel current  $I_{ion}$  is much

smaller than the other components,  $I_{ion}$  can be neglected in Eq. (1). Therefore, the EP current  $I_{EP}(t)$  at any time  $t$  can be determined as follows:

$$I_{EP}(t) = I_{tot}(t) - I_{Leak}(t) \quad (2)$$

provided that the total current  $I_{tot}(t)$  can be directly measured and  $I_{Leak}(t)$  can be determined in a certain way.

Here, we will employ electrochemical impedance spectroscopy (EIS) to obtain an equivalent circuit model for the calculation of leakage current  $I_{Leak}$ . This model can be used to predict the leakage current for the poration medium (without cells) and cell suspension. It can be shown that the EP current can be related to the electropore dynamic process. In addition, the resealing procedure was also examined and the resealing time constants were determined for different pulse treatments.

## 2. Methods

### 2.1. Device fabrication

Micro EP chips with three-dimensional gold micro electrodes were fabricated by using Microelectromechanical System (MEMS) technology and a modified electroplating process. A gold seed layer was patterned first using the lift-off technique, so that no additional step was required to etch the gold layer in an iodide bath after electroplating. This can prevent the electroplated structure from being attacked, and ensures that it is consistent with the original design. The detailed fabrication process was described elsewhere [6]. A photograph of a packaged micro EP chip and the SEM close-up view of the fabricated 3D electrode structures are shown in Fig. 2.

### 2.2. Cell preparation

Human cervical cancer cells (HeLa cell) were grown as a monolayer in a 60 mm Petri dish in EMEM medium (CCL-2™, ATCC, VA, USA), supplemented with 10% fetal bovine serum (ATCC, VA, USA) at 37 °C and 5% CO<sub>2</sub>. Cells were trypsinized by 0.05% trypsin/EDTA and then were washed twice with the poration medium (comprised of 280 mM mannitol, 5 mM sodium phosphate, 10 mM potassium phosphate, 1 mM MgCl<sub>2</sub> and 10 mM HEPES at the pH level of 7.4) by spinning at

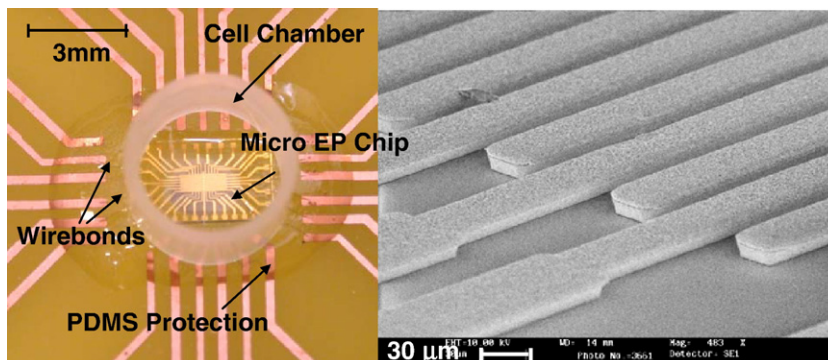


Fig. 2. A photo of a packaged micro EP chip (left) and the SEM close-up view of the 3D microelectrodes (right).

1400 rpm at room temperature. Subsequently, they were re-suspended in the poration medium at a high concentration of  $10^8$  cells/mL. The purpose of using high concentration cell suspension was to block the space between the two electrodes and minimize the current bypassing the cell.

### 2.3. Impedance spectroscopy

Electrochemical method has been widely adopted in biological applications [14]. The electrical impedance measurements can be used to build an equivalent circuit to describe the electric characteristics of the system.

The impedance measurement setup consisted of a two-electrode system, where one of the multiple-input electrodes was used as a working electrode and a common ground as a counter electrode. Counter electrode and reference electrode from the instrument were connected to each other. In the experiments, 15  $\mu$ L poration medium and HeLa cell suspension ( $10^8$  cells/mL) were loaded onto the micro EP chip respectively. Electrochemical impedance spectroscopy (EIS) was carried out with Autolab PGSTAT 30 Potentiostat/Galvanostat system (Eco Chemie, the Netherlands) with frequency response analyzer (FRA) using a modulation voltage of 10 mV. The scanning frequency ranged from 10 Hz to 100 kHz at zero bias potential.

### 2.4. Current response during EP

The experimental setup for recording cells' current response was built as shown in Fig. 3. A sequence of pulses with increasing

pulse amplitude ranging from 1 V to 6 V were delivered to micro EP chip by one HP 33120A function generator. A 1 k $\Omega$  high precision resistor connected in series with the micro EP chip functions as a current to voltage converter. The resistance of this 1 k $\Omega$  resistor is far smaller than that of chip circuit so that it can be ignored in current analysis. Real-time voltage signal from this resistor was then recorded simultaneously by using PCI 6110 DAQ card (National Instrument, TX, USA) for further analysis. The sampling frequency was kept at 1 MHz.

### 2.5. Resealing dynamics after EP

Resealing kinetics of cell suspension was examined by using a series of low-voltage short pulses with 1 V amplitude, 1 ms pulse duration and 50 ms pulse intervals immediately after the high intensity pulse (stimulation pulse) treatment. The change of measured current responses with time can indicate the conductivity change as a function of time which reflects cell membrane resealing procedure.

## 3. Determine electroporation current to reveal electropore dynamics

### 3.1. Building an equivalent circuit model for the system to predict the leakage current

The current responses  $I_{\text{tot}}$  of 15  $\mu$ L poration medium and cell suspension on a microchip recorded at a sequence of 0.2 ms pulses with increasing pulse amplitude ranging from 1 V to 6 V

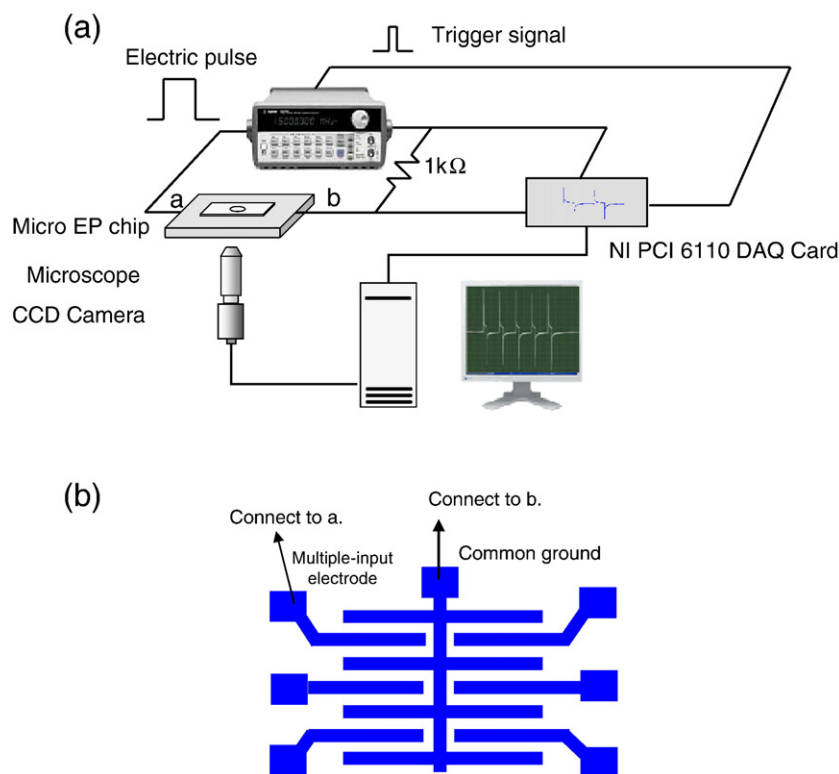


Fig. 3. (a) Experimental setup for the micro electroporation system, (b) the layout of the micro EP chip and the interconnection of the micro electrodes in the experimental setup.

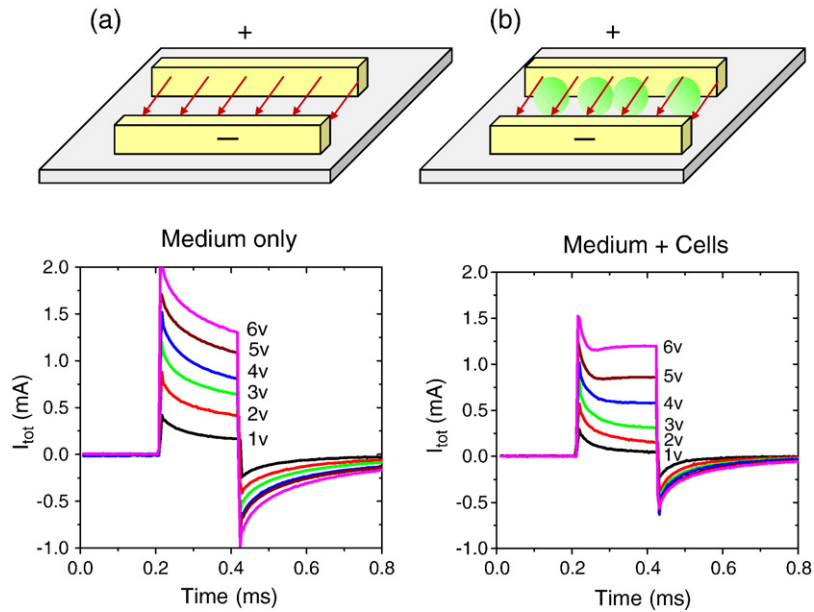


Fig. 4. Current responses,  $I_{\text{tot}}$ , to different input electric pulses ranging from 1 V to 6 V for (a) the poration medium, (b) HeLa cell suspension. Average electric field can be calculated by  $E_{\text{avg}} = \alpha U_a / L_e$ , where  $\alpha = 0.976$  and  $L_e = 30 \mu\text{m}$ .

was shown in Fig. 4. An average electric field can be obtained by averaging the non-uniform electric field distribution calculated from the numerical simulation [6]. Therefore, the externally applied voltage  $U_a$  can be converted to the average electric field  $E_{\text{avg}} = \alpha U_a / L_e$  via a correction factor  $\alpha = 0.976$ , where  $L_e$  is the

distance between the two adjacent electrodes. It is obvious that the current measured in the poration medium is larger than the current in the cell suspension, since the cells act as a lossy dielectric object in the intact state to block the current passing across the two electrodes. At an applied voltage larger than 3 V, it

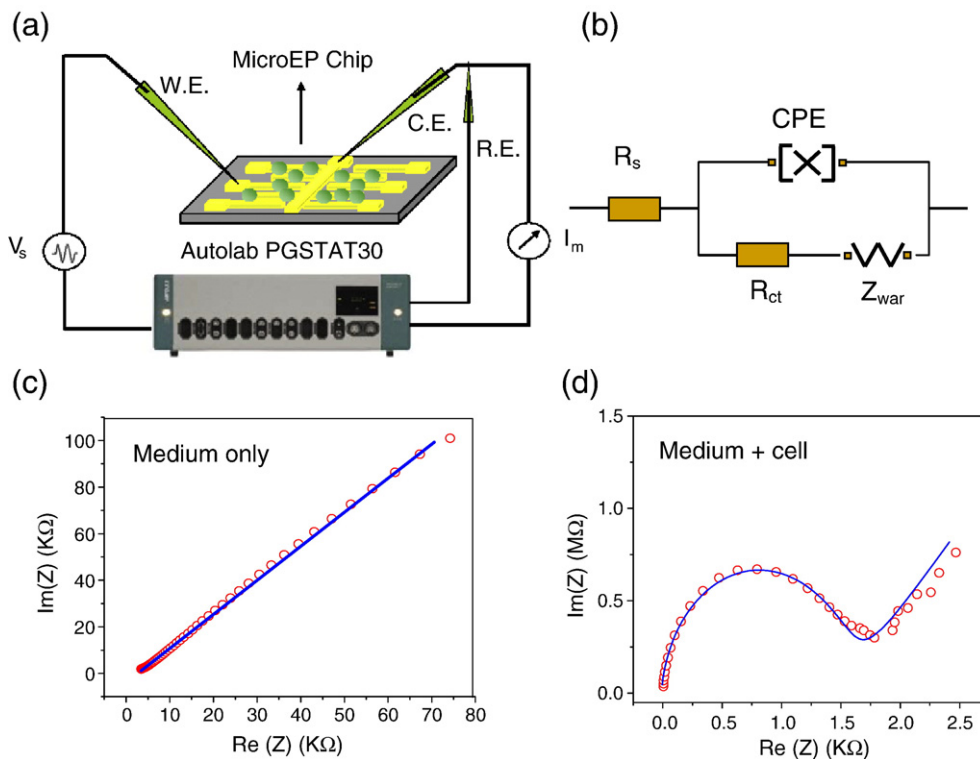


Fig. 5. (a) Electrochemical impedance spectroscopy setup: R.E.=Reference Electrode, W.E.=Working Electrode, C.E.=Counter Electrode, CPE=Constant Phase Element. (b) Equivalent circuit used to model the impedance data. Fitted (solid line) and experimental (open circle) Nyquist plots of impedance spectra in poration medium (c) and cell suspension (d) at zero potential. Frequency ranges from 10 Hz to 100 kHz.



can be seen that there is a current “jump” in cell suspension (Fig. 4(b)). The current jump is due to the increase of cell membrane conductance. Since HeLa cells are not excitable, the ion-channel current can be negligible [14]. Thus, if the undesired leakage current can be isolated from the total current response, the dynamics of membrane conductance changes can be characterized by using electroporation current data.

To build an equivalent circuit model for the system, electrochemical impedance spectroscopy was carried out with Autolab PGSTAT 30 at a range of 10 Hz to 100 kHz. The electrodes of microchip and Autolab system were connected as shown in Fig. 5(a). In this electrode configuration, we can measure the impedance of the poration medium or the cell suspension in between the common ground electrode and the multiple-input electrode. Therefore, we obtained the Nyquist plots for the impedance for the poration medium on the microchip (Fig. 5(c)) and for the cell suspension on the microchip (Fig. 5(d)). The Nyquist plots display the polar plot of the impedance,  $Z(\omega)$ , as a function of frequency  $\omega$  in the complex plane. The Nyquist plot can be formed by plotting the imaginary part of  $Z(\omega)$  against the real part of  $Z(\omega)$  at different frequencies.

Based on these Nyquist plots, a modified Randle’s equivalent circuit [15] as shown in Fig. 5(b) was found to nicely fit the impedance data over the working frequency range (the solid lines in Fig. 5(c) and (d)). The equivalent circuit consists of four components which are defined by five parameters.  $R_{ct}$  is a charge transfer resistance and CPE is a Constant Phase Element,  $Z_{CPE} \equiv 1/(Y_0 j\omega)^n$ , which can be determined by two parameters,  $Y_0$  and  $n$ . The phase angle of CPE impedance is independent of the frequency and has a value of  $(-90 \times n)$  degrees.  $Z_{war}$  represents the Warburg impedance associated with diffusive ion transport and  $R_s$  is the resistance of electrolyte between the two electrodes [15]. All of the five parameters for the poration medium (PM) and cell suspension,  $R_s$ ,  $Y_0$ ,  $n$ ,  $R_{ct}$  and  $W_0$  were determined and further adjusted by a short pulse for system calibration. (see more detail in the supplementary data) (Fig. 6).

### 3.2. Electroporation current determination

The net electroporation currents  $I_{EP}$  can be determined by Eq. (2), i.e., subtracting the leakage current  $I_{Leak}$  from the measured total current response of the cell suspension  $I_{tot}$ . The  $I_{Leak}$  can be determined by the numerical calculation from the equivalent circuit model using Laplace transform and Inverse Laplace Transform (see the Supplementary data for detailed information). As shown in Fig. 7(a)–(c), the EP currents under different electric pulses (amplitude from 1 V to 6 V and the pulses duration of 0.2 ms, 0.8 ms and 2 ms) were recorded.

Similar to the result previously obtained from fluorescence microscopy with Propidium Iodide (PI) dye indicator [6], the EP current can only be detected when external applied voltage is larger than some critical value, e.g. 3 V pulse with duration of 0.2 ms and 2 V pulse with duration of 0.8 ms and 2 ms. The threshold voltage indicates the minimum voltage to induce conductivity increase of cell membrane under different pulse duration. And the longer the pulse duration, the lower the pulse

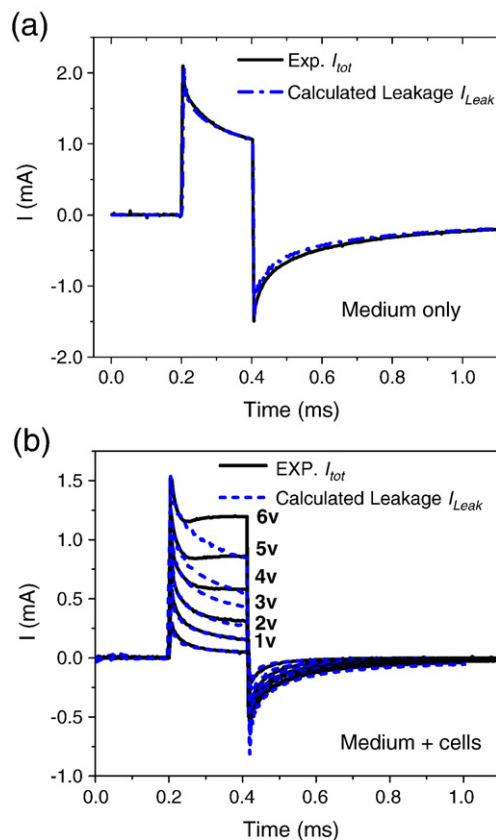


Fig. 6. (a) Measured current response  $I_{tot}$  of the poration medium (black solid line) and calculated leakage current response  $I_{Leak}$  (blue dash dot) at  $U = 6$  V and  $t_d = 0.2$  ms. (b)  $I_{tot}$  of cell suspension (solid line) and calculated leakage current response  $I_{Leak}$  (dash line) at a sequence of 0.2 ms pulses with increasing pulse amplitude ranging from 1 V to 6 V. Average electric field can be calculated by  $E_{avg} = \alpha U_a / L_c$ .

amplitude required for a detectable EP current. The isolated EP currents under the same voltage of 6 V with pulse duration of 0.2, 0.8 and 2 ms were plotted in Fig. 7(d). It can be seen that the EP current increased at the same rate for the three pulse widths.

### 3.3. Electroporation formation time constant

Although the nanoscale pores can only be observed on cell membrane by rapid-freezing electron microscope 1 ms after pulse treatment [16], we believe that the conductivity increase at hundreds of micro seconds is the precursor of pore formation by using small molecule fluorescent dye, propidium iodide. We can monitor the free diffusion of dye molecules through electropores (Fig. 9(a)). The EP current measurement and fluorescent microscopy are in good agreement at the threshold voltage which induces cell membrane permeability.

As shown in Fig. 9(b), EP current increase undergoes two stages, a rapid increase Region 1 followed by a more flat Region 2. Region 1 is related to the initiation of a large number of small pores induced by the external electric field, while Region 2 shows the further expansion of these pores. The time constant of electropore formation was then defined by the intersection point of the tangent lines of Region 1 and that of Region 2 since most

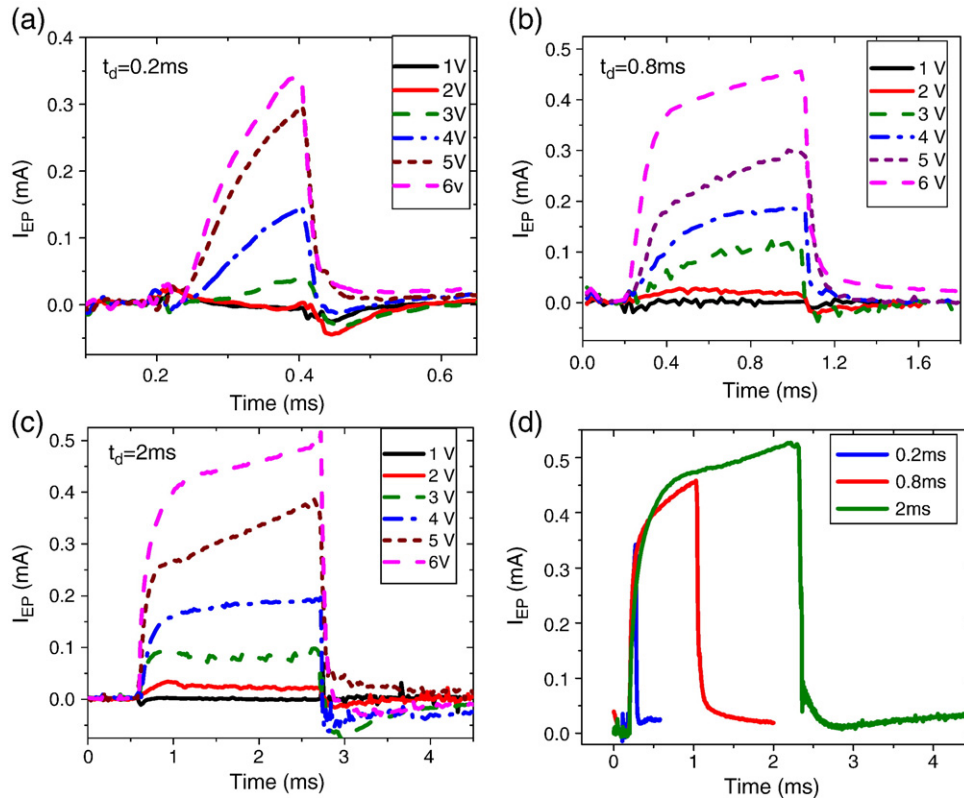


Fig. 7. The EP current  $I_{EP}$  on the micro EP chip for the case of cell suspension was determined under the pulse amplitude of 1–6 V and pulse duration (a) 0.2 ms, (b) 0.8 ms (c) 2 ms, and (d) EP currents under different pulse widths of 6 V. Average electric field can be calculated by  $E_{avg} = \alpha U_a / L_c$ .

of pores have been generated in Region 1. The electroporation time constants under different pulse amplitudes and pulse duration of 0.8 ms and 2 ms were listed in Table 1.

#### 4. Resealing dynamics and time constant determination

The resealing current  $I_{reseat}$  can be defined as the difference between the measured current responses after simulation pulse treatments  $I_{tot}$  and the predicted current from equivalent circuit  $I_{Leak}$ . It indicates the conductivity change as a function of time which reflects cell membrane resealing procedure. Due to the electric pulse induced pores on the cell membrane, the resealing current reached its peak value immediately after the stimulation pulse treatment and decrease gradually with time. The resealing time constant is the time elapsed after the conductivity of cell membrane decays to 37% ( $1/e$ ) of the peak value immediately after the stimulation pulse treatment. By integrating the resealing current, the total charge across the permealized membrane can be calculated as follows:

$$Q_i = \int_{t=t_i}^{(t_i+1)\text{ms}} i_{reseat}(t) dt \quad (3)$$

where  $t_i$  is the starting time of the  $i$ -th pulse with the amplitude of 1 V and 1-ms pulse duration,  $i=1,2,\dots,250$ . With the aid of  $Q_i$ , the cell membrane recovery dynamics can then be examined and the resealing time constant can be determined.

Fig. 8 shows the comparison of the total charge  $Q_i$  as a function of time obtained from both of the poration medium and cell suspension after the treatment of a 6-volt pulse with the duration of 0.2 ms. The total charge data obtained from cells suspension (solid line) can be fitted by dual exponential decay function

$$Y_0 + A_1 \exp(-t/\tau_1) + A_2 \exp(-t/\tau_2), \quad (4)$$

which consists of a short time constant  $\tau_1$  and a long time constant  $\tau_2$ . The short time constant  $\tau_1$  was related to the electric pulse induced ion accumulation at the two electrodes surface and consequently the change of the electric double layer. This type of quick current recovery phenomenon can also be seen in poration medium, as dash dot line shown in Fig. 8, which has a very short time constant of 0.092 s, similar to  $\tau_1$  in 0.087 s. The long time constant  $\tau_2$  was related to cell membrane recovery. The resealing time constant for the treatment of a 6-volt electric pulse with duration of 200  $\mu$ s is around 1.54 s. After

Table 1  
The time constants of electroporation for different pulse treatments

Pulse amplitude					
Pulse width	2 V	3 V	4 V	5 V	6 V
800 $\mu$ s	585 $\mu$ s	410 $\mu$ s	343 $\mu$ s	265 $\mu$ s	189 $\mu$ s
2 ms	625 $\mu$ s	453 $\mu$ s	370 $\mu$ s	278 $\mu$ s	200 $\mu$ s

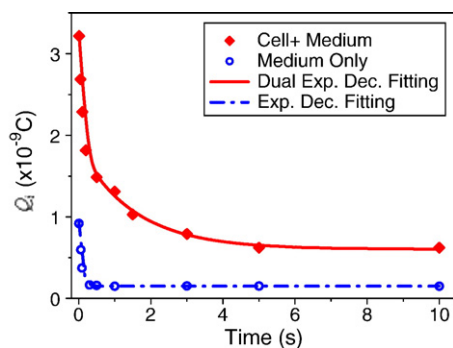


Fig. 8. The total charge of cell suspension and poration medium after the treatment of a 6-volt pulse with the duration of 200  $\mu$ s. In cell suspension (solid line) the short time constant  $\tau_1=0.087\pm 0.013$  and long time constant  $\tau_2=1.540\pm 0.211$  while in poration medium (dash dot)  $\tau=0.092\pm 0.006$ . Average electric field can be calculated by  $E_{\text{avg}}=\alpha U_a/L_c$ .

analyzing the EP current under different electric pulse treatments, the cell membrane recovery time constants have been determined as listed in Table 2.

## 5. Discussion

The recorded current response of HeLa cells during an electrical pulse consists of several components. Since HeLa cells are not excitable, the ion-channel current can be negligible. Thus the leakage currents which include the membrane capacitance current and currents bypassing cells were the only major components need to be extracted. This paper presents a novel method to predict the leakage current and then extract the EP current, which reflects the dynamics of cell membrane electroporation.

By measuring EP current we can detect the cell membrane electroporation threshold, above which membrane permeabilization occurs. While higher than critical electric field, short pulse widths required higher electric field intensities and vice versa (as shown in Fig. 7).

The threshold voltages of EP obtained from current measurement show in good agreement with fluorescent microscopy results (Fig. 9(a)). Moreover, current measurement provides a method with time resolution down to ns (1  $\mu$ s in our experiment) which can not be achieved by a common CCD video camera, while fluorescent microscopy can verify the current increase is related to pores formation and also provides the information about the size of pores. A micro electroporation chip made it possible to carry out the two methods simulta-

Table 2  
Cell membrane recovery time constants for different stimulation pulse treatments (in seconds)

Pulse amplitude	Pulse width		
	4 V	5 V	6 V
200 $\mu$ s	0.8123 $\pm$ 0.1054	1.2906 $\pm$ 0.08112	1.5403 $\pm$ 0.2106
800 $\mu$ s	1.0475 $\pm$ 0.1980	1.3999 $\pm$ 0.1018	1.6700 $\pm$ 0.1395
2 ms	1.5076 $\pm$ 0.1106	1.9097 $\pm$ 0.1808	2.1700 $\pm$ 0.1981

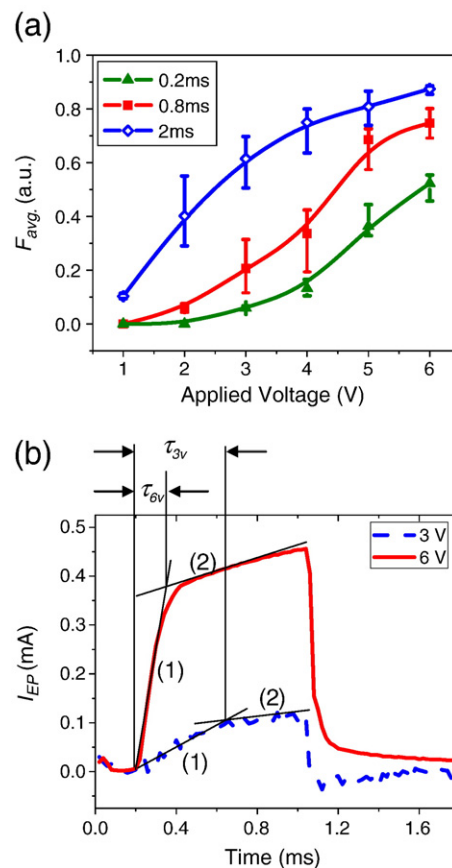


Fig. 9. (a) Average fluorescence intensity of propidium iodide,  $F_{\text{avg}}$ , as a function of applied voltage with duration of 0.2 ms, 0.8 ms and 2 ms. Each data point from the average of 10 single HeLa cells and (b) the definition of the time constant of electropore formation. Average electric field can be calculated by  $E_{\text{avg}}=\alpha U_a/L_c$ .

neously. The conductivity increase during electric pulse was also reported on densely packed pellets of CHO cells [17] and on a single HeLa cell trapped in a micro channel [18].

As listed in Table 1, the electropore formation time constant, decreased from around 400  $\mu$ s for 3 V to 200  $\mu$ s for 6 V while the EP current increased at the same rate under the same applied voltage but different pulse width (Fig. 7(d)). This is because the transmembrane potential of spherical cells is estimated by  $V(t)=1.5Ea\cos\theta [1-e^{-t/\tau_m}]$ , where  $E$  is the electric-field intensity,  $a$  is the radius of the cell,  $\theta$  is the polar angle measured with electric field  $E$ , and  $\tau_m$  is the membrane charge time constant. For a high electric intensity, the time required for charging the membrane to the critical transmembrane potential (around 1 V) is shorter than a lower one. Thus, the slope of current increase is large at a higher applied voltage. Besides, the peak current depended on pulse duration at the same pulse amplitude. Longer pulse duration results in higher peak current due to a group of larger pores on the cell membrane. Fig. 7(d) shows the EP current at three different pulse widths under the same applied voltage of 6 V. The current increased under the same slope at the beginning due to the same pore initiation rate. After 200  $\mu$ s, the current increase was slowed down. This can be contributed the

fact that the formation of many small pores will cause the decrease in membrane potential. This membrane potential decrease can decrease the formation of new pores.

In conclusion, pulsed electric field initiated short-lived structural changes in the cell membrane can be detected by observing the EP current. As shown in [Table 1](#) all the three pulse amplitude with 2 ms pulse width needs a recovery time longer than 1.5 s, while a high amplitude pulse with short pulse width (6 V and 200  $\mu$ s) can be more quickly recovered. If a high electrical field for a relatively long time was exposed to cells, it eventually will lead to the cell lysis and the membrane cannot be repaired anymore. The recovery time we obtained here were consistent with the single-cell measurement results by Khine et al. [19].

In their experiments, single-cell was trapped by a micro-channel and the conductivity change of membrane was recorded by Ag/AgCl electrodes and a patch-clamp amplifier. The averaged resealing time constants for various pulse conditions were at around 1.75 s.

## 6. Conclusion

Micro electroporation chips with 3D micro electrodes have been designed and fabricated, using MEMS technology and a modified electroplating process. A nonlinear equivalent circuit, with the help of impedance measurement, was proposed for the dynamic study of micro electroporation on microchips. Undesired leakage currents bypassing the cells on the microchip were predicted by the equivalent circuit modeling and simulation. The increase of electroporation current due to electroporation and the time constant of the electropore formation have been successfully determined under different input voltages and pulse duration. Cell membrane recovery dynamic was also examined and the resealing time constants were determined for different pulse treatments. This provides an alternative efficient method to quantify the temporal changes in cell membrane conductance and electropores in response to electroporation.

## Acknowledgement

This work is supported by Hong Kong Research Grants Council (project ref no. 616205).

## Appendix A. Supplementary data

Supplementary data associated with this article can be found, in the online version, at [doi:10.1016/j.bioelechem.2008.01.007](https://doi.org/10.1016/j.bioelechem.2008.01.007) [20,21].

## References

[1] E. Neumann, M. Schaefer-Ridder, Y. Wang, P.H. Hofschneider, Gene transfer into mouse lymphoma cells by electroporation in high electric fields, *EMBO J.* 1 (1982) 841–845.

- [2] D.C. Chang, B.M. Chassy, J.A. Saunders, A.E. Sowers, *Guide to Electroporation and Electrofusion*, Academic Press, San Diego, 1992, pp. 1–6.
- [3] K. Kinoshita, T.Y. Tsong, Formation and resealing of pores of controlled sizes in human erythrocyte membrane, *Nature* 268 (1977) 438–441.
- [4] D.C. Bartoletti, G.I. Harrison, J.C. Weaver, The number of molecules taken up by electroporated cells: quantitative determination, *FEBS Lett.* 256 (1989) 4–10.
- [5] H. Liang, W.J. Purucker, D.A. Stenger, R.T. Kubinieć, S.W. Hui, Uptake of fluorescence-labeled dextrans by 10 T 1/2 fibroblasts following permeation by rectangular and exponential-decay electric field pulse, *Biotechniques* 6 (1988) 550–558.
- [6] H. He, D.C. Chang, Y.-K. Lee, Using a micro electroporation chip to determine the optimal physical parameters in the uptake of biomolecules in HeLa cells, *Bioelectrochemistry* 71 (2006) 80–85.
- [7] I.G. Abidor, V.B. Arakelyan, L.V. Chemomordik, Yu.A. Chizmadzhev, V.E. Pastushenko, M.R. Tarasevich, Electric breakdown of bilayer lipid membranes I. The main experimental facts and their qualitative discussion, *Bioelectrochem. Bioenerg.* 6 (1979) 37–52.
- [8] M. Schmeer, T. Seipp, U. Pliquett, S. Kakorin, E. Neumann, Mechanism for the conductivity changes caused by membrane electroporation of CHO cell-pellets, *Phys. Chem. Chem. Phys.* 6 (2004) 5564–5574.
- [9] T. Griese, S. Kakorin, E. Neumann, Conductometric and electrooptic relaxation spectrometry of lipid vesicle electroporation at high fields, *Phys. Chem. Chem. Phys.* 4 (2002) 1217–1227.
- [10] K. Kinoshita, T.Y. Tsong, Voltage-induced conductance in human erythrocyte, *Biochim. Biophys. Acta.* 554 (1979) 479–497.
- [11] F. Ryttsen, C. Farre, C. Brennan, S.G. Weber, K. Nolkrantz, K. Jardemark, D.T. Chiu, O. Orwar, Characterization of single-cell electroporation by using patch-clamp and fluorescence microscopy, *Biophys. J.* 79 (2000) 1993–2001.
- [12] H. Krassen, U. Pliquett, E. Neumann, Nonlinear current–voltage relationship of plasma membrane of single CHO cells, *Bioelectrochemistry* 70 (2007) 71–77.
- [13] T.R. Gowrishankar, W. Chen, R.C. Lee, Non-linear microscale alterations in membrane transport by electroporation, *Ann. N. Y. Acad. Sci.* 858 (1998) 205–216.
- [14] J. Seo, C. Ionescu-Zanetti, J. Diamond, R. Lal, L.P. Lee, Integrated multiple patch-clamp array chip via lateral cell trapping junctions, *Appl. Phys. Lett.* 84 (2004) 1973–1975.
- [15] E. Barsoukov, et al., *Impedance spectroscopy: theory, experiment, and applications*, Wiley-Interscience, Hoboken, N.J., 2005.
- [16] D.C. Chang, *Electroporation and electrofusion*, in: R.A. Meyers (Ed.), *Encyclopedia of molecular cell biology and molecular medicine*, vol. 4, Wiley-VCH Publishers, Weinheim, Germany, 2004, pp. 135–137.
- [17] M. Schmeer, T. Seipp, U. Pliquett, S. Kakorin, E. Neumann, Mechanism for conductivity changes caused by membrane electroporation of CHO cell-pellets, *Phys. Chem. Chem. Phys.* 6 (2004) 5564–5574.
- [18] M. Khine, A. Lau, C. Ionescu-Zanetti, J. Seo, L.P. Lee, A single cell electroporation chip, *Lab Chip* 5 (2005) 38–43.
- [19] M. Khine, C. Ionescu-Zanetti, A. Blatz, L.-P. Wang, L.P. Lee, Single-cell electroporation arrays with real-time monitoring and feedback control, *Lab Chip* 7 (2007) 457–462.
- [20] B.S. Garbow, G. Giunta, J.N. Lyness, A. Murli, Software for an implementation of Weeks' method for the inverse of the Laplace Transform, *ACM TOMS* 14 (1988) 163–170.
- [21] J.A.C. Weideman, Algorithms for parameter selection in the weeks method for inverting the Laplace Transform, *SIAM J. Sci. Comput.* 21 (1999) 111–128.